

# Simulation and analysis of two-point bending fatigue test of asphalt concrete based on discrete element model

Cao Qingqing<sup>1</sup> Liu Xiuyu<sup>1</sup> Wang Hao<sup>2</sup> Huang Xiaoming<sup>1</sup>

(<sup>1</sup>School of Transportation, Southeast University, Nanjing 210096, China)

(<sup>2</sup>Department of Civil and Environmental Engineering, Rutgers, State University of New Jersey, Piscataway, NJ 08854, USA)

**Abstract:** In order to investigate the fatigue performance of French high modulus asphalt concrete and the correlation between Burger's parameters and fatigue life, the virtual model of asphalt mixture trapezoidal specimen in the two-point bending fatigue test was constructed in discrete element software PFC3D. The initial stiffness and the maximum stress when the specimen reached fatigue were calculated. Through the comparison between virtual and single field fatigue test curves, the credibility of simulation in DEM was verified. Then, the impacts of top controlled displacement and Burger's parameters ( $E_1$ ,  $E_2$ ,  $\eta_1$ ,  $\eta_2$ ) on the fatigue life of the specimen were explored. The simulation results indicate that the maximum stress increases with the increase in the top controlled displacement. With the increase of  $E_1$  and the decrease of  $E_2$  in Burger's model, the modulus of the asphalt binder increases, and the fatigue performance of the asphalt mixture enhances.  $\eta_1$  and  $\eta_2$  have limited influence on fatigue life compared with  $E_1$  and  $E_2$ .

**Key words:** high modulus asphalt concrete; numerical simulation; Burger's parameters; fatigue life

**DOI:** 10.3969/j.issn.1003-7985.2017.03.006

High modulus asphalt binder (HMAB) with a penetration grade less than 25 (0.1 mm) at 25 °C has played a pivotal role in the French asphalt mixture design method<sup>[1]</sup>. After being developed in the France for over 30 years, it was introduced to the United Kingdom, South Africa and Australia<sup>[2]</sup>. The superiority of high modulus asphalt concrete (HMAC) mainly lies in its better performance in deformation, fatigue and moisture resistance than base asphalt<sup>[3]</sup>.

Research conducted by Corté<sup>[4]</sup> in 2001 indicated that HMAC showed better anti-fatigue performance and an increment in strain after fatigue failure. Hernández<sup>[5]</sup> reported that high modulus asphalt retained good resistance to

fatigue and rutting. Airey et al.<sup>[6]</sup> evaluated the aging and moisture induced damage resistance of HMAC through laboratory tests. Previous studies proved the engineering potentiality of this material but failed to reveal the mechanism for improving fatigue performance<sup>[3, 7-8]</sup>. Thus, numerical simulations based on the finite element method (FEM) were conducted to investigate the mechanical responses and road performance of this material. Zhang et al.<sup>[9]</sup> simulated the distribution of maximum deflection and shear stress for HMAC pavement under the standard axle load in 2012. Zheng et al.<sup>[10]</sup> evaluated the permanent deformation of HMAC using the finite element method. However, the assumption of homogeneity of asphalt concrete in FEM was not able to accurately reflect the material properties.

Compared with FEM, the discrete element method (DEM) is superior for investigating the micromechanics asphalt mixture and in describing the dynamics of the assembly of aggregates and asphalt binder. In 2001, Ullidtz<sup>[11]</sup> simulated the permanent deformation and brittle damage of asphalt mixture after repeated loading using DEM. Buttlar et al.<sup>[12]</sup> investigated the indirect shear test by conducting a virtual test on the discrete element model. Liu et al.<sup>[13]</sup> tested and verified the effectiveness of Burger's model in simulating the mechanical behaviors of asphalt. Chen et al.<sup>[14]</sup> studied the fatigue test of asphalt mixture using PFC and verified the modeling method through the comparison of simulation and laboratory results. Thus, DEM is selected to investigate the fatigue performance of HMAC.

In this paper, a virtual three-dimensional trapezoidal specimen model was constructed in PFC3D, a particle flow software based on DEM. Then, Burger's model was applied to describe the viscoelastic properties of the asphalt binder. The virtual model was verified through the comparison with laboratory fatigue test results. Then, the fatigue performance of the virtual specimen was evaluated by verified top controlled displacement and Burger's model parameters. As a result, the connection between the fatigue performance of HMAC and the viscoelastic properties of the asphalt binder was established. This study provides a new insight and theoretical basis for improving the fatigue performance of asphalt mixture using HMAC design.

**Received** 2016-12-05.

**Biographies:** Cao Qingqing (1993—), female, graduate; Huang Xiaoming (corresponding author), male, doctor, professor, huangxm@seu.edu.cn.

**Foundation item:** The National Natural Science Foundation of China (No. 51378121).

**Citation:** Cao Qingqing, Liu Xiuyu, Wang Hao, et al. Simulation and analysis of two-point bending fatigue test of asphalt concrete based on discrete element model[J]. Journal of Southeast University (English Edition), 2017, 33(3): 286 – 292. DOI: 10.3969/j.issn.1003-7985.2017.03.006.

## 1 Development of DEM Model

### 1.1 Virtual 3D trapezoidal specimen

Two-point trapezoidal beam fatigue test is widely adopted in Europe to evaluate the fatigue performance of asphalt mixture. According to European standard BS EN 12697-24<sup>[15]</sup>, the test is conducted in the controlled displacement mode (see Fig. 1). In the test, the base surface of the specimen is fixed to the device platform using epoxy resin. Simultaneously, constant amplitude sinusoidal deflection  $D$  shown in Fig. 2 is exerted on the top surface of the specimen horizontally. Fatigue failure is reached when the recorded force on the top surface decreases to a certain percentage of the initial value.

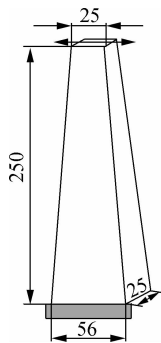


Fig. 1 Two-point trapezoidal beam(unit: mm)

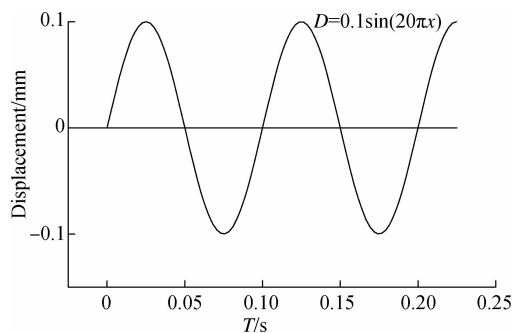


Fig. 2 Applied sinusoidal displacement

Asphalt mixture is a three-phase composite material composed of the asphalt binder, aggregates and voids. Since fine aggregates and mineral fines have minor contribution to the mixture's strength and move with the asphalt binder under external force, the aggregates smaller than 4 mm, mineral fines and asphalt binder are assumed to be homogeneous discrete elements in PFC.

Based on the asphalt mixture composition shown in Tab. 1<sup>[16]</sup>, coarse aggregates, asphalt binder and voids were generated in PFC3D. The asphalt content was 6.4%, and air voids were 4%. The entire process of generating a virtual three-dimensional trapezoidal specimen of asphalt mixture in PFC is shown in Fig. 3. In the first step, coarse aggregates were generated as aggregate balls without overlapping in the trapezoidal volume (see Fig. 3(a)). Then, 1 mm ball units were created evenly in the whole trape-

zoidal volume, overlaying the space of the aggregates (see Fig. 3(b)). These balls represent the asphalt binder and 1 mm was proved to be the most suitable size<sup>[14]</sup>. Afterwards, irregular polyhedron aggregates were created by applying the clumps generating algorithm in PFC based on the position information in Fig. 3(a). The algorithm considered the center of each aggregate ball to be the centroid of the external cube, and several random planes were generated to cut the hexahedral to obtain irregular polyhedron aggregate. The homogeneous 1 mm balls included in the polyhedron aggregates were regarded as part of an aggregate element, and then were cumulated together as "clump" unit in PFC. There was no contact among balls in the clump, which were a suitable replacement for the aggregates. Then, the aggregates generated in Fig. 3(a) were deleted, and thus there was no overlapping in the three-dimensional specimen. The eventually obtained virtual specimen shown in Fig. 3(c) contained two phases: aggregates represented by clumps and asphalt binder represented by 1 mm ball units. In order to meet the requirements of air voids in the asphalt mixture, the numbers of ball units calculated according to the volume fraction were deleted at random. It was assumed that all the air voids in the virtual specimen were distributed randomly.

Tab. 1 Asphalt mixture gradation

Sieve size/mm	4	6.3	10	14
Percentage/%	31.5	55	76	100

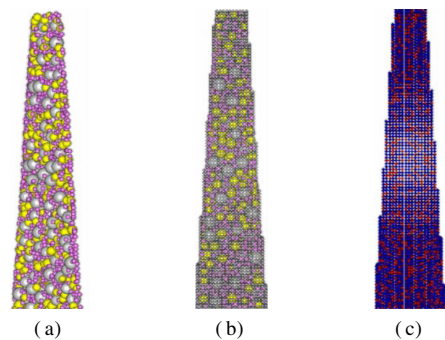


Fig. 3 Construction of the virtual trapezoidal specimen in PFC. (a) Coarse aggregates; (b) Ball units; (c) Clumps and ball units

### 1.2 Microscopic contact parameters

Four types of microscopic contact parameters are taken into consideration in the following models: the elastic contact and point bond model among the interior units of aggregates, the rheological and parallel bond model among the interior units of asphalt binder, the rheological and parallel bond model between aggregates and asphalt binder, and the elastic contact and parallel bond model between different aggregates. As the "clump" was applied to describe the aggregates and the force inside the clump was ignored, contact among the interior units of aggregates was also ignored in this paper. The contact model between the aggregates and asphalt binder is equiv-

alent to the contact among the interior units of asphalt binder, due to the binder film covering the aggregates.

The physical properties of aggregates have a high stability, and thus the elastic modulus and Poisson's ratio can be chosen as the constant. The parallel bond model contains normal and tangent stiffness parameters  $K_n$  and  $K_s$ , which are only concerned with the radius of discrete units. Corresponding microscopic parameters are shown in Tab. 2.

**Tab. 2** Microscopic contact model parameters of aggregate

$E/\text{GPa}$	$\mu$	$K_n/(\text{MN} \cdot \text{m}^{-1})$	$K_s/(\text{MN} \cdot \text{m}^{-1})$
55	0.25	222R	55.5R

Notes:  $E$  is the elastic modulus;  $\mu$  is Poisson's ratio;  $R$  is the radius of discrete units.

The rheological contact model has an important role in describing the mechanical properties of asphalt binder. Burger's model was chosen as a good approximation for macroscopic mechanics. The creep compliance of the model is expressed as

$$J(t) = \frac{1}{E_1} + \frac{t}{\eta_1} + \frac{1}{E_2^{1-\exp(-\frac{t}{\tau})}} \quad (1)$$

The corresponding microcosmic Burger's model in PFC is equivalent to the viscoelastic beam between two elements with a radius of  $R_1$  and  $R_2$ . The equivalent beam length is  $L = R_1 + R_2$ . The microscopic Burger's model can be represented in normal and tangent directions individually in Fig. 4<sup>[17]</sup>.  $C_{mn}$ ,  $K_{mn}$ ,  $C_{kn}$ ,  $K_{kn}$ ,  $C_{ms}$ ,  $K_{ms}$ ,  $C_{ks}$ , and  $K_{ks}$  are the microscopic Burger's parameters.

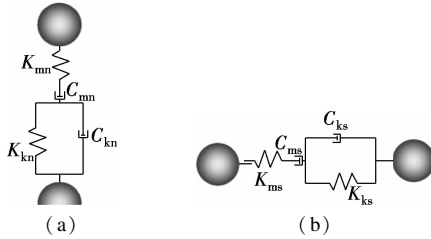


**Fig. 4** Microscopic Burger's model. (a) Normal; (b) Tangent

Supposing that the micro-contact force is  $f_n$ , the relationship between  $f_n$  and macro-contact stress  $\sigma$  is  $f_n = \sigma A$ , where  $A = L^2$  is the cross sectional area of the equivalent beam. The normal micro-contact force can be expressed as

$$f_n = \dot{\varepsilon}_{mc} C_{mn} L = L \dot{\varepsilon}_k K_{km} + L \dot{\varepsilon}_k C_{kn} = \dot{\varepsilon}_{mk} K_{mn} L \quad (2)$$

where  $\varepsilon_{mn}$ ,  $\varepsilon_k$ ,  $\varepsilon_{mk}$  are the corresponding strains for the mechanical elements in Burger's model.

The macro-contact stress can be expressed as

$$\sigma = \dot{\varepsilon}_{mc} \eta_1 = \dot{\varepsilon}_k E_2 + \dot{\varepsilon}_k \eta_2 = \dot{\varepsilon}_{mk} E_1 \quad (3)$$

Combining Eqs. (2), (3) and  $f_n = \alpha A$ , the normal parameters of microscopic Burger's model can be written as

$$\begin{aligned} C_{mn} &= \eta_1 L, & K_{mn} &= E_1 L \\ C_{kn} &= \eta_2 L, & K_{kn} &= E_2 L \end{aligned} \quad (4)$$

Considering that the relationship between elastic modulus

$E$  and shear modulus is  $G = \frac{E}{2(1+\mu)}$ , the tangent parameters of microscopic Burger's model can be written as

$$\begin{aligned} K_{ks} &= \frac{E_2}{2(1+\mu)} L, & C_{ks} &= \frac{\eta_2}{2(1-\mu)} L \\ K_{ms} &= \frac{E_1}{2(1+\mu)} L, & C_{ms} &= \frac{\eta_1}{2(1-\mu)} L \end{aligned} \quad (5)$$

The microscopic Burger's model parameters can be selected once the macroscopic Burger's model is determined. Komba et al.<sup>[18]</sup> performed the laboratory dynamic modulus testing for hot-mix asphalt with a 20/30 penetration grade binder, which satisfied the HMAB definition. Thus, the microscopic Burger's model is determined according to the relationship between micro and macro parameters. The microscopic rheological parameters of asphalt mixture are shown in Tab. 3.

**Tab. 3** Microscopic contact model parameters of asphalt

Parameter	$C_{mn}$	$K_{mn}$	$C_{kn}$	$K_{kn}$	$C_{ms}$	$K_{ms}$	$C_{ks}$	$K_{ks}$
Value	267 852L	17 034L	184L	31 016L	107 141L	6 814L	74L	12 406L

Based on the model parameters above, a two-point trapezoidal fatigue test was simulated in PFC. The test was carried out with a top displacement amplitude of 0.1 mm and loading frequency of 10 Hz. Applied force on the top of the trapezoidal specimen was recorded every 10 cycles. The field two-point trapezoidal fatigue test was conducted and the loading force was recorded as well<sup>[16]</sup>.

According to the conventional bending theory, the stiffness modulus of HMAC in two-point bending fatigue tests has the following expression<sup>[19]</sup>:

$$E = w \frac{l}{\delta_0 db} \left[ \frac{K_1 l^2}{d^2} + K_2 (1 + \mu) \right] \quad (6)$$

where  $w$  is the applied load, kN;  $l$  is the length of the specimen, m;  $\delta_0$  is the deflection at the top, mm;  $d$  is the top width, m;  $b$  is the thickness of the specimen, m;  $K_1$  and  $K_2$  are the coefficients depending on the geometry of the specimen,  $K_1 = 0.37064$ ,  $K_2 = 1.14402$ .

Based on the recorded loading force in the simulation and field tests, the stiffness variations of trapezoidal specimen are calculated and plotted in Fig. 5. Observing the

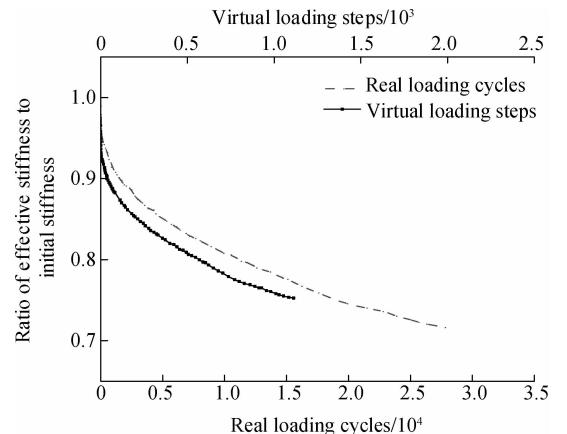


**Fig. 5** Variation of stiffness in the field test and simulation test

two curves, an identical tendency is detected among the simulation results and realistic results. The comparison can confirm the validity of the microscopic parameters adopted in the virtual DEM model.

## 2 Results and Analysis

### 2.1 Virtual fatigue test realized in PFC

In the virtual model, the position of the base layer of ball units in the trapezoid specimen was fixed. The constant amplitude sinusoidal deflection applied to the top layer horizontally was changed to 1 mm. Loading frequency was chosen as 10 Hz, which meant that loading time was around 0.016 s. The maximum stress inside the specimen is recorded utilizing serro-mechanism.

In the field bending fatigue failure, fatigue failure is reached when the force on the top of the specimen declines to 50% of the initial force. However, it is time consuming to adopt that criteria. Thus, it was considered that the specimen fails when the force on the top of the specimen declines to 60% of the initial force. The simulation result is of the same significance as it reflects the same tendency of the fatigue life variation when the parameters change.

As can be seen from Fig. 6, the applied force on the specimen dropped rapidly, and then gradually tended to be smooth with cycling. As the crack did not occur in the deflection-control fatigue test, the decrease of the maximum stress follows a similar tendency.

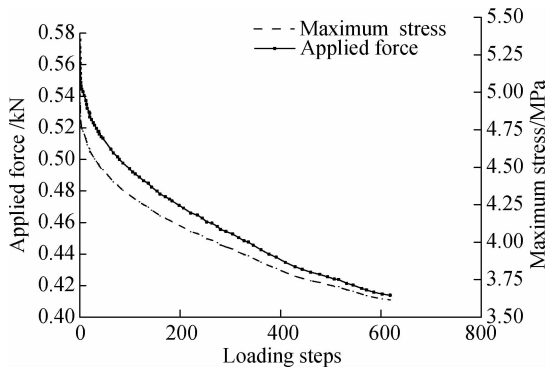


Fig. 6 Applied force and maximum stress vs. loading steps

### 2.2 Effect of top displacement on fatigue life

In the simulations, by altering the displacement applied to the top of the specimen, with the frequency being maintained, the values of fatigue life and the maximum stresses were observed. The initial stiffness was calculated by Eq. (6).

Fig. 7 shows that when the displacement increases, the fatigue life decreases, and the maximum stress increases. It can be seen that the variation of fatigue life is nearly linear with deflection after the logarithmic coordinate is applied. From Eq. (6), it can be seen that when the stiffness remains, the applied force linearly increases with

deflection increasing. This is related to the increasing maximum stress in the specimen. The multiples of deflection amplification are related to the maximum stress increasing multiples. If the applied deflection is increased tenfold, the maximum stress increases approximately tenfold at the same time. Ignoring the decimal omission due to the scientific notation, this can be attributed to the fact that the maximum strain in the specimen is linear with macro deflection, and the strain is related to the applied deflection.

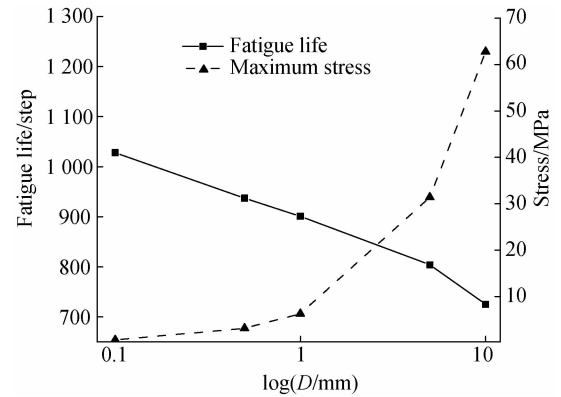


Fig. 7 Variations of fatigue life and stiffness vs. controlled deflection

The stiffness remains constant in the test, which is around 4 GPa, and it is independent of applied deflection.

### 2.3 Effects of macroscopic parameters on fatigue life

As the viscoelastic property of the asphalt binder has an important role in enhancing the modulus of asphalt mixture, it is necessary to investigate the effects of rheological parameters to provide a theoretical basis for improving the fatigue performance of the asphalt mixture.

The viscoelastic property of asphalt mixture is expressed by Burger's model in this paper, and macroscopic mechanical parameters ( $E_1, E_2, \eta_1, \eta_2$ ) in the model have a close correspondence with microscopic parameters ( $C_{mn}, K_{mn}, C_{kn}, K_{kn}, C_{ms}, K_{ms}, C_{ks}, K_{ks}$ ) as above. Thus, the determination of  $E_1, E_2, \eta_1, \eta_2$  is important for reflecting material mechanical properties.

When different grades of asphalt are selected in the mixture, usually most of macroscopic parameters are changed, particularly when high modulus asphalt mixture is taken into analysis. It is discovered that  $E_1$  tends to increase and  $E_2$  tends to decrease when the asphalt modulus rises and penetration drops. In order to investigate the influence of macroscopic parameters ( $E_1, E_2, \eta_1, \eta_2$ ) in Burger's model on the fatigue life of asphalt mixture, the method of control variables is applied in this part. The maximum displacement on the top of the specimen is 0.1 mm, and the frequency applied is 10 Hz.

Based on the simulation results in Fig. 8, the fatigue life of the asphalt mixture increases when  $E_1$  increases.

This shows high degree of consistency with field test results. It is found from the simulation that the maximum stress increases with the increase of  $E_1$ . And, according to Eq. (6), the initial stiffness increases from 6 800 to 10 220 MPa with the increase of  $E_1$ . The results indicate a completely different trend of the variation of  $E_2$  compared with  $E_1$ . It explained why the fatigue life and maximum stress decreases with the increase of  $E_2$ , and the calculated initial stiffness drops from 4 445 to 3 625 MPa, which corresponds to the previous study<sup>[20]</sup>. The effects of  $E_1$  and  $E_2$  are opposite, and the high modulus of HMAC can be attributed to the increase of  $E_1$ .

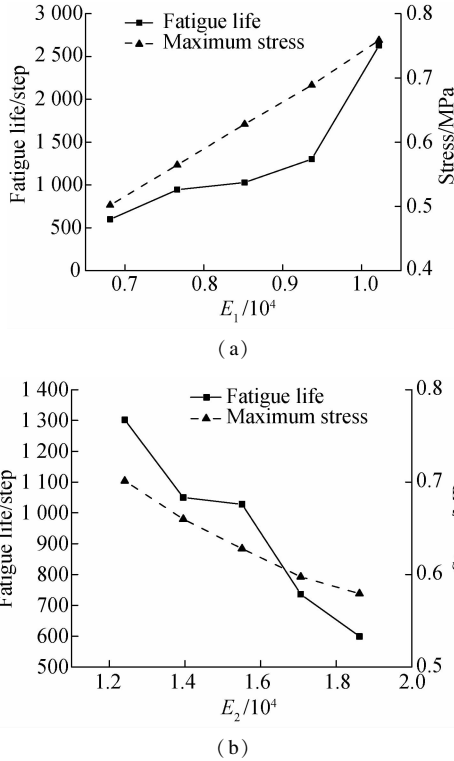


**Fig. 8** Variations of fatigue life and stiffness. (a) Variable  $E_1$ ; (b) Variable  $E_2$

Only when  $\eta_1$  and  $\eta_2$  vary simultaneously, the fatigue life changes but follows no pattern (see Fig. 9). What is interesting in Fig. 9 is when  $\eta_1$  increases, regardless of

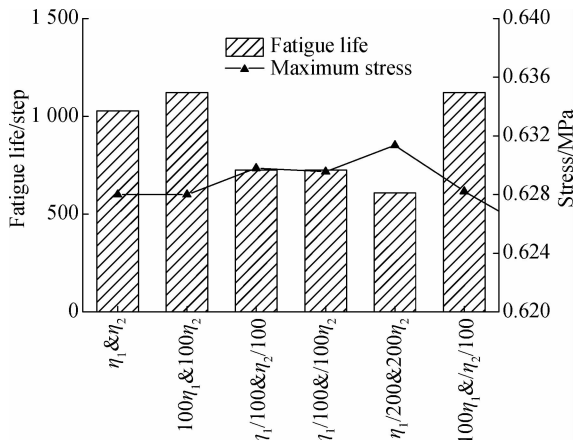


**Fig. 9** Variations of fatigue life and stiffness vs. viscosity

the increase or decrease of  $\eta_2$ , the fatigue life climbs, and vice versa. Compared to  $E_1$  and  $E_2$ ,  $\eta_1$  and  $\eta_2$  impact less on fatigue life and only cause an obvious variation after enlarging 100 times. As the initial stiffness varies from 3 951 to 3 959 MPa, the effects on the initial stiffness and maximum stress can be both ignored. Thus, although  $\eta_1$  and  $\eta_2$  do not influence the stiffness of the material, they affect the fatigue life to a limit.

## 2.4 Evaluation of high modulus asphalt

From above, when the asphalt modulus increases and the penetration grade decreases,  $E_1$  tends to increase, while  $E_2$  tends to decrease, and  $\eta_1$  and  $\eta_2$  vary diversely, which is in accordance with the previous study<sup>[21]</sup>. To simulate the characteristics of high modulus asphalt, four parameters were changed simultaneously. The virtual experimental results above show that the effects of  $\eta_1$  and  $\eta_2$  on fatigue life are negligible compared with  $E_1$  and  $E_2$  under equivalent amplification. Thus, different scaling factors were applied to the parameters.

Next, a new situation is taken into consideration:  $\eta_1$  is expanded to 100 times, with  $E_1$  to 1.15 times and  $E_2$  to 0.95 times. Fatigue life increased from 1 208 to 2 628, while initial stiffness and maximum stress increased from 3 959 and 628 to 4 049 and 648, respectively. It is clear that the life of a high modulus asphalt mixture specimen is prolonged.

According to Lee et al.<sup>[22]</sup>, adopting high modulus asphalt to improve fatigue life was demonstrated through field tests. The results in this paper verified the conclusion based on the discrete element method, and explained the performance of high modulus asphalt mixture in the rheological level of Burger's parameters that  $\eta_1$ ,  $E_1$  and  $E_2$  are related to the variation of fatigue life.

## 3 Conclusions

1) In this paper, a virtual three-dimensional trapezoidal specimen of asphalt mixture was established in PFC. Based on the virtual model, two-point trapezoidal bending fatigue test was conducted on the specimen. The model was verified with the comparison between simulating and laboratory test results. Then, the fatigue performance of the specimen was evaluated with verified top controlled displacement and Burger's model parameters.

2) In a single virtual fatigue test, the force applied on the top of the specimen reduced rapidly and then slowed down to a balanced value eventually. Stiffness and maximum stress decreased simultaneously.

3) With the increase of the applied displacement, the fatigue life of the specimen declined. And, the fatigue life of the virtual specimen increased when the Burger's model parameters  $E_1$  were enhanced and  $E_2$  reduced. The parameters  $\eta_1$  and  $\eta_2$  have less impact on the fatigue life of the specimen. The stiffness of the material mainly con-

tributes to the increase of  $E_1$  and the decrease of  $E_2$ . Thus, HMAC with higher stiffness has longer fatigue life.

4) In general, high modulus asphalt with lower penetration grade is recommended in this paper to improve the fatigue life of asphalt mixture, and this can be applied to extend the life of the asphalt pavement in road engineering.

## References

- [1] Diefenderfer B K, Maupin G W Jr. Field trials of high-modulus high-binder-content base layer hot-mix asphalt mixtures[J/OL]. *Biotechniques*, 2010, **27**(3). <https://trid.trb.org/view.aspx?id=986723>.
- [2] Denneman E, Petho L, Verhaeghe B, et al. High modulus asphalt (EME) technology transfer to South Africa and Australia; Shared experiences[C/OL]//*Conference on Asphalt Pavements for Southern Africa*. Pilanesberg, South Africa, 2015. [http://researchspace.csr.co.za/dspace/bitstream/handle/10204/8248/Verhaeghe\\_2015.pdf?sequence=1&Allowed=y](http://researchspace.csr.co.za/dspace/bitstream/handle/10204/8248/Verhaeghe_2015.pdf?sequence=1&Allowed=y).
- [3] Geng H, Clopotel C S, Bahia H U. Effects of high modulus asphalt binders on performance of typical asphalt pavement structures[J]. *Construction and Building Materials*, 2013, **44**: 207 – 213. DOI: 10.1016/j.conbuildmat.2013.03.035.
- [4] Corté J F. Development and uses of hard-grade asphalt and of high-modulus asphalt mixes in France[J]. *Transportation Research Circular*, 2001, **503**: 12 – 31.
- [5] Hernández M I G. High modulus asphalt concrete: A long life asphalt pavement[J/OL]. *Journal of Civil & Environmental Engineering*, 2015. <http://dx.doi.org/10.4172/2165-784X.1000188>. DOI: 10.4172/2165 – 784x.1000188.
- [6] Airey G D, Choi Y K, Collop A C, et al. Combined laboratory ageing/moisture sensitivity assessment of high modulus base asphalt mixtures (with discussion)[C]//2005 *Journal of the Association of Asphalt Paving Technologists: From the Proceedings of the Technical Sessions*. Long Beach, CA, USA, 2005, **74**:307 – 345.
- [7] Ma T, Wang H, Huang X M, et al. Laboratory performance characteristics of high modulus asphalt mixture with high-content RAP[J]. *Construction and Building Materials*, 2015, **101**: 975 – 982. DOI: 10.1016/j.conbuildmat.2015.10.160.
- [8] Benta A, Duarte C, Almeida-Costa A, et al. Design and performance of a warm high-modulus asphalt concrete[J]. *Journal of Cleaner Production*, 2015, **95**: 55 – 65. DOI:10.1016/j.jclepro.2015.02.057.
- [9] Zhang X N, Yang P. Finite element analysis of high modulus asphalt pavement[J]. *International Journal of Advancements in Computing Technology*, 2012, **4**(2): 72 – 79.
- [10] Zheng M L, Han L L, Qiu Z P, et al. Simulation of permanent deformation in high-modulus asphalt pavement using the Bailey-Norton creep law[J]. *Journal of Materials in Civil Engineering*, 2016, **28**(7):04016020. DOI: 10.1061/(asce)mt.1943 – 5533.0001511.
- [11] Ullidtz P. Distinct element method for study of failure in cohesive particulate media[J]. *Transportation Research Record: Journal of the Transportation Research Board*, 2001, **1757**:127 – 133. DOI:10.3141/1757-15.
- [12] Buttlar W, You Z. Discrete element modeling of asphalt concrete: Microfabric approach[J]. *Transportation Research Record: Journal of the Transportation Research Board*, 2001, **1757**:111 – 118. DOI:10.3141/1757-13.
- [13] Liu Y, Dai Q L, You Z P. Viscoelastic model for discrete element simulation of asphalt mixtures[J]. *Journal of Engineering Mechanics*, 2009, **135**(4): 324 – 333. DOI:10.1061/(asce)0733-9399(2009)135:4(324).
- [14] Chen J, Huang X M. Simulation of fracture process of asphalt mixture using three-dimension discrete element method[J]. *Journal of South China University of Technology(Natural Science Edition)*, 2012, **40**(7): 21 – 26. (in Chinese)
- [15] British Standards Institution. BS EN 12697-24 Bituminous mixtures—test methods for hot mix asphalt—Part 24:Resistance to fatigue[S]. London: European Committee for Standardization, 2004.
- [16] Bodin D, de La Roche C, Chabot A. Prediction of bituminous mixes fatigue behavior during laboratory fatigue tests[C]//*Proceedings of the 3rd Eurasphalt and Eurobitume Congress*. Vienna, Austria, 2004: 1935 – 1945.
- [17] Cheng J, Zhang D, Huang X M. *Application of discrete element particle flow software in road engineering*[M]. Beijing:China Communications Press, 2015: 110 – 114. (in Chinese)
- [18] Komba J J, Maina J W, Anochie-Boateng J K, et al. Analytical modelling of visco-elastic behaviour of hot-mix asphalt[C/OL]//*Southern African Transportation Conference*. Pretoria, South Africa, 2012. [https://researchspace.csr.co.za/dspace/bitstream/handle/10204/6037/Komba\\_2012.pdf?sequence=1&Allowed=y](https://researchspace.csr.co.za/dspace/bitstream/handle/10204/6037/Komba_2012.pdf?sequence=1&Allowed=y).
- [19] Cocurullo A, Airey G D, Collop A C, et al. Indirect tensile versus two-point bending fatigue testing[J]. *Proceedings of the Institution of Civil Engineers—Transport*, 2008, **161**(4): 207 – 220. DOI: 10.1680/tran.2008.161.4.207.
- [20] He X Y, Yan J H. The application of high modulus asphalt technology[J]. *Transpo World*, **2009**(7): 182 – 189. (in Chinese)
- [21] Wu J W, Bai Y F, Collop A C, et al. Numerical simulation of uniaxial compression test for asphalt mortar with discrete element method[J]. *Highway*, **2012**(3): 193 – 197. (in Chinese)
- [22] Lee H J, Lee J H, Park H M. Performance evaluation of high modulus asphalt mixtures for long life asphalt pavements[J]. *Construction and Building Materials*, 2007, **21**(5): 1079 – 1087. DOI: 10.1016/j.conbuildmat.2006.01.003.

# 基于 DEM 的沥青混凝土两点弯曲疲劳试验模拟分析

曹青青<sup>1</sup> 刘修宇<sup>1</sup> 汪 浩<sup>2</sup> 黄晓明<sup>1</sup>

(<sup>1</sup> 东南大学交通学院, 南京 210096)

(<sup>2</sup>Department of Civil and Environmental Engineering, Rutgers, State University of New Jersey, Piscataway, NJ 08854, USA)

**摘要:**为了研究法国高模量沥青混凝土疲劳性能及 Burger’s 模型参数与疲劳寿命之间的关系,在离散元软件 PFC3D 中建立了沥青混凝土锥棱柱两点疲劳弯曲试验的虚拟模型. 计算了虚拟试件的初始刚度及达到疲劳时的最大接触应力,并与实测单次疲劳试验曲线对比,验证了用 DEM 模拟疲劳试验的可行性. 然后研究端部位移及 Burger’s 模型中各项参数( $E_1, E_2, \eta_1, \eta_2$ )对疲劳寿命的影响. 数值模拟结果表明,随着端部控制位移增大,到达疲劳时最大应力增大. 研究证实:随着沥青砂浆 Burger’s 模型参数中  $E_1$  增大,  $E_2$  减小, 沥青模量增大, 沥青混合料的疲劳寿命得到有效提升;  $\eta_1$  和  $\eta_2$  对疲劳寿命的影响较小.

**关键词:**高模量沥青混凝土;数值模拟;Burger’s 参数;疲劳寿命

**中图分类号:**U416.2